

# INFERENCE OF GEOACOUSTIC MODEL PARAMETERS FROM ACOUSTIC FIELD DATA

**N. Ross Chapman**

School of Earth and Ocean Sciences, University of Victoria, Victoria, BC V8P5C2, Canada

chapman@uvic.ca

The interaction of sound with the ocean bottom has a significant impact on the acoustic field in the ocean, especially in shallow water. Over the past several decades, there has been a high level of research activity in ocean acoustics to understand the physics of sound propagation in the ocean bottom. This work has led to the general practice of using geoacoustic models, - profiles of the sound speed, attenuation, and density of ocean bottom materials  $\tilde{n}$  to describe the bottom. Much of the research was focused on developing inversion methods to determine geoacoustic model parameter values from the information about the model contained in measurements of the acoustic field  $\tilde{n}$  or quantities that can be derived from the field  $\tilde{n}$  in the water. This paper reviews the stages in the development of geoacoustic inversion as a statistical inference process to estimate geoacoustic model parameter values and their associated uncertainties. Applications of linear inversions and non-linear inversions based on matched field processing are presented for analysis of their performance in estimating realistic geoacoustic models. The paper concludes by pointing out limitations in the present day inversion techniques that can severely limit performance, and discusses some new approaches that provide robust performance without compromising the accuracy of the estimated model parameters.

## INTRODUCTION

Accurate representation of the acoustic field in the ocean is fundamentally important for many applications in ocean acoustics, from traditional naval interests in evaluating sonar performance to present day environmental concerns in assessment of the impact of anthropogenic sound sources on marine life. The measured field from a sound source in the ocean is uniquely determined by the physical conditions of temperature and salinity in the water, and the depth and geoacoustic properties of the ocean bottom. The mapping between the physical properties of the ocean waveguide and the acoustic field is non-linear, and the relationship is expressed by the acoustic wave equation [1, 2]. In all but a few simplified ocean waveguide models, analytic solution of the wave equation is not possible and sophisticated numerical techniques such as ray theory approximations, normal mode methods, wave number integral methods and parabolic equation approximations have been developed for calculating the field in realistic ocean waveguide environments [2]. These methods have been tested extensively in benchmarking sessions against simulated waveguide environments of varying complexity, and are in widespread use for applications with experimental data.

Solution of the wave equation involves satisfying boundary conditions of pressure release at the sea surface, and continuity of pressure and vertical particle velocity at the ocean bottom for the conventional assumption that the bottom is a fluid system; if the bottom is an elastic solid, there is an additional constraint of continuity of horizontal stress. The effect of the bottom on the acoustic field in the water is significant, particularly in shallow water environments, and there has been considerable research effort to understand the physics of sound propagation in ocean bottom materials. The interaction of sound with the ocean bottom is described in calculations of the acoustic field

using geoacoustic models of the physical bottom structure that generally consist of profiles in depth, range and cross-range of the sound speed,  $c$ , attenuation,  $\alpha$ , and density,  $\rho$ , of the bottom materials. In most cases, the cross-range variation is negligible, but range dependence of the profiles in depth is common. Knowledge of these physical properties is necessary for constructing geoacoustic models that will enable accurate representation of the field. An example of a simple geoacoustic model is shown in Figure 1; the form of this model is typical of those used for applications with experimental data.

The geoacoustic model in the figure does not explicitly include shear wave parameters. Although shear wave effects in elastic solid material can be modelled in most numerical propagation codes, the impact of shear wave losses is not significant in most shallow water environments that consist of fine-grained, high porosity sediment material in which the shear wave speed near the sea floor is very low ( $< 300$  m/s). Consequently, in most of the geoacoustic inversions reported in the literature, the bottom is modelled as a fluid. Exceptions to this approach include shallow or deep water environments where elastic solid material is found relatively close (within a few wavelengths) to the sea floor, e.g. calcarenite and limestone sea bottom regions off the west coast of Australia, and thin-sediment basalt regions of the Pacific Ocean. In those environments, the shear wave speed is comparable to or greater than the sound speed in water, and so the coupling with the compressional wave generated in the water is very strong. Inversions of data from such environments must take account of shear wave propagation in the bottom.

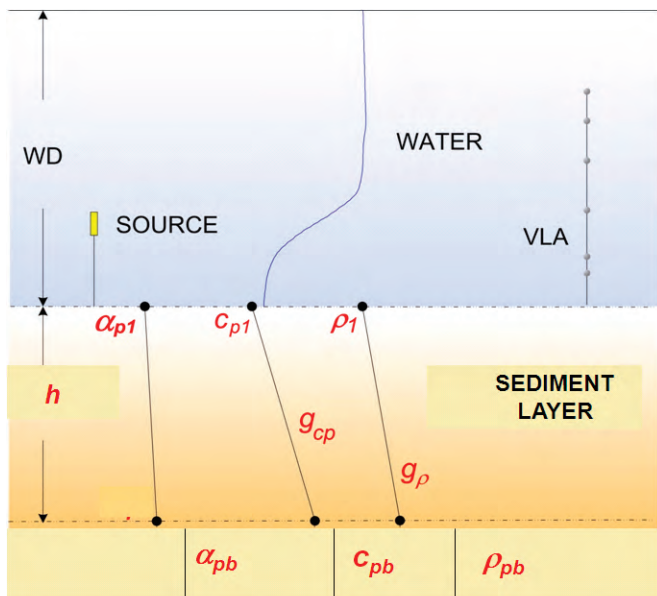


Figure 1. Geoacoustic model consisting of a simple layered structure of sound speed,  $c$ , attenuation,  $\alpha$ , and density,  $\rho$

The sensitivity of the acoustic field to geoacoustic model parameters was recognised many years ago by researchers who noted that improvements in modelling transmission loss data [3] and bottom loss data [4] could be obtained by adjusting specific model parameters. The simplicity of the approach is very appealing, and it continues to be applied in some studies [5]. However, an approach to inversion by changing model parameters in a trial and error fashion is highly subjective, and there is no measure of the uncertainty of the parameter value that provides the best fit to the data. More importantly, it ignores the sensitivities and the impact of errors in other model parameters that are held at fixed values. A more systematic approach of iteration over forward models was suggested by Frisk [6], but the computation time in executing such a grid search over many geoacoustic model parameters was and remains prohibitively long.

Over the past twenty years, there has been considerable interest in ocean acoustics in developing objective inversion techniques to estimate geoacoustic model parameters from measurements of the acoustic field – or quantities that can be derived from the acoustic field – in the water [7]. This approach using remote acoustic sensing is attractive because it is an efficient means for characterising the ocean bottom over large areas, and the estimates are made on material in its natural setting. By comparison, estimates based on point measurements that involve analysis of physical samples of the bottom material are expensive and time consuming, and may introduce additional problems in making measurements in other than *in situ* conditions. However, as will be seen later, the general practice is to compare the inferences from inversions to ground truth data from physical samples or other *in situ* measurements.

The inversion methods fall into two main categories, linear methods that assume small changes from an initial profile, and methods that are fully non-linear [8]. Linear inverse

problems are described by a well-established analytical theory that provides measures of the resolution and variance of the estimated parameters [9], and they have the additional appealing advantage of being computationally very fast. The non-linear methods are examples of model-based signal processing techniques that were made possible by the introduction of efficient numerical techniques for exploring multi-dimensional model parameter spaces. Inversion methods based on both approaches have been benchmarked in exercises with simulated data [10, 11], and have also been applied for use with data from experiments in many different ocean bottom environments - with varying degrees of success.

This paper reviews the stages in the development of geoacoustic inversion as a statistical inference process. The next section describes the background for the inverse problem, and describes some initial attempts in ocean acoustics to estimate geoacoustic parameters from experimental data. Linear inverse methods are then introduced, with examples of applications that use wave number measurements to infer the sound speed profile in marine sediment. Following this, non-linear model-based inversion is introduced with a discussion of matched field processing, followed by a description of inversion by Bayesian inference and demonstration of its performance with examples of applications to experimental data.

## GEOACOUSTIC INVERSION METHODS

### Inverse problems

Inversion can be described as the process of inferring information about a physical system from measurements of physical quantities that result from an interaction with the system. For geoacoustic inversion, this statement translates roughly as: given measurements of the acoustic field that has interacted with the bottom, what information can be inferred about the properties of the ocean bottom that generated the measured data? It might be expected that the inversion provides estimates of the material properties and structure of the real ocean bottom. However, this is not the case. Inversion provides the estimates of the parameters of a geoacoustic model that is designed to represent the bottom. Since the model is never exactly the true ocean bottom and since the data contain errors, the inverse problem is inherently non-unique. In the inversion process, we are comparing measured data with calculated replicas of the data based on the parameters of the designed geoacoustic model, and there are many different models that will provide very good fits to the data. One of the most significant challenges is designing an appropriate model, whether this is done by judicious choice based on prior information about the bottom structure, or within the inversion process itself.

Formally, the inverse problem in ocean acoustics is developed in terms of the relationship through the wave equation between the model parameters  $\mathbf{m} = [m_1, m_2, \dots, m_M]^T$  and the measured data  $\mathbf{d} = [d_1, d_2, \dots, d_N]^T$ . The model parameters may be sound speeds, attenuations, densities and thicknesses of sediment layers. The primary physical quantity is the sound pressure, which can be measured directly with hydrophones in experiments. However, other quantities that are derived from

the pressure field such as horizontal wave numbers of normal modes; bottom reflection loss; modal amplitudes; modal dispersion and particle velocity are also used; travel time of received signals is also a useful quantity.

Measured data contain noise  $\mathbf{n}$  that is assumed to be additive:  $\mathbf{d} = \mathbf{d}_0 + \mathbf{n}$ . The vector  $\mathbf{d}_0$  is the data predicted by the wave equation that would be obtained in an ideal, perfectly accurate experiment in which the ocean waveguide is described by the set of model parameters  $\mathbf{m}$ :

$$\mathbf{d}_0 = F(\mathbf{m}) \quad (1)$$

As mentioned above, this problem has a unique and stable solution. The inverse problem of inferring the set of model parameters that generated the data is expressed by

$$\mathbf{m} = F^{-1}(\mathbf{d}) \quad (2)$$

This problem is very difficult to solve, if a solution exists. Existence is usually addressed by constructing a geoacoustic model that provides an adequate fit to the data, within some specified uncertainty. However, the solution is non-unique, due to incomplete or inaccurate data, and is generally unstable—small errors in the data can lead to large changes in the estimated model parameter values. The complete solution to the inverse problem must provide both a set of estimated values and their associated uncertainties.

It is worthwhile to stress here what is meant by data errors. Errors can arise from two different sources: measurement errors that are due to inaccurate readings or ambient noise, and theory errors due to inaccurate or incomplete parameterisation of the geoacoustic model or approximations in the physics of the forward propagation problem. The data errors are not known explicitly, and it is usually assumed that  $\mathbf{d}$  is a random variable with a Gaussian distribution. The theory errors are more difficult to estimate, and they can be the dominant source of uncertainty in the inversion.

### Linearised inversion

Although the relationship between the pressure and the geoacoustic model parameters is non-linear, linear relationships can be developed for some observables that are derived from the acoustic field. In this approach, the problem is linearised in the vicinity of a reference model  $\mathbf{m}_0$ , and it is assumed that the unknown model is related to the reference model by a small perturbation. Perturbation inversion has the advantage of the fast computational speed of linear methods, but there are many problems that offset this advantage. The most serious concern is that one is never sure that the final model is independent of the reference model. In many cases, the inversion does not converge if the starting model is not close to the solution, or more likely, it converges to a local minimum. Another serious issue is that because the relationship is nonlinear, it can be very misleading to use only the parameter space near the final estimated model to characterise the solution. Nevertheless, if used carefully, the approach can generate remarkably useful models.

An outstanding example of perturbation inversion was reported by Frisk et al. who developed an elegant method

for estimating sound speed profiles in marine sediments by linearising the relationship between changes in the horizontal wave numbers of propagating modes and changes in the sound speed [12, 13]. The method assumes a background model for the sound speed profile  $c_0(z)$  that generates a set of horizontal wave numbers  $k_{0m}$  and corresponding modal functions  $Z_{0m}(z)$  for a sound frequency  $\omega$  that are solutions of the depth-separated wave equation,

$$\left( \rho_0(z) \frac{d}{dz} \left( \frac{1}{\rho_0(z)} \frac{d}{dz} \right) + k_0^2(z) \right) Z_{0m}(z) = k_{0m}^2 Z_{0m}(z) \quad (3)$$

where  $\rho_0(z)$  is the density profile. The true model is thus

$$c(z) = c_0 + \delta c(z) \quad (4)$$

and the wave numbers are changed from those for the background model,

$$k(z) = \omega / (c_0(z) + \delta c(z)) \quad (5)$$

Applying first-order perturbation theory, an approximation can be obtained for the change in wave number with respect to that for the background model in terms of the change in sound speed [13]

$$\delta k_m = k_m - k_{0m} = \frac{1}{k_{0m}} \int_0^\infty |Z_{0m}(z)|^2 \frac{k_0^2(z) \delta c(z)}{\rho_0(z) c_0(z)} dz \quad (6)$$

For a discretely sampled sound speed profile in depth, (6) can be cast in terms of a linear relationship between  $\delta k(z)$  and the geoacoustic model parameters,

$$\delta k = \mathbf{Gm} \quad (7)$$

where  $G$  is a  $N \times M$  matrix consisting of the background sound speed, density and mode functions;  $N$  is the number of discrete samples of the sound speed profile, and  $M$  is the number of model parameters [13].

Application of the method requires estimation of the horizontal wave numbers of propagating modes. The basis for this is the Hankel transform relationship between the depth-dependent Green's function and measurements of the variation of pressure with range for a specific sound frequency [12]. Good results have been obtained for experimental data from range independent waveguides, and an extension of the technique for range dependent waveguides using a short-time Fourier transform was developed by Becker [14]. Figure 2 shows an example of wave number estimation using this technique applied to data from the Shallow Water '06 (SW06) experiment that was carried out on the New Jersey continental shelf [15]. The estimated wave numbers of eight modes that are resolved in the data change slightly with the increasing water depth along the track. The estimated value of mode 6 is sensitive to a slow speed layer that pinches out and disappears towards the end of the track (Figure 3).



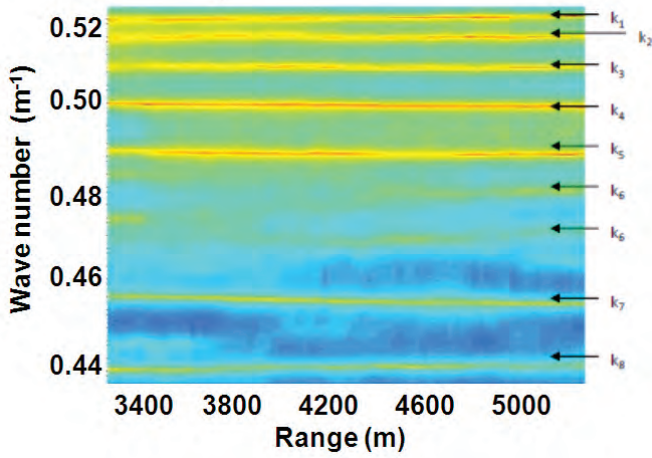


Figure 2. Modal wave numbers of 8 propagating modes that were estimated from SW06 experimental data of sound pressure versus range for a frequency of 125 Hz

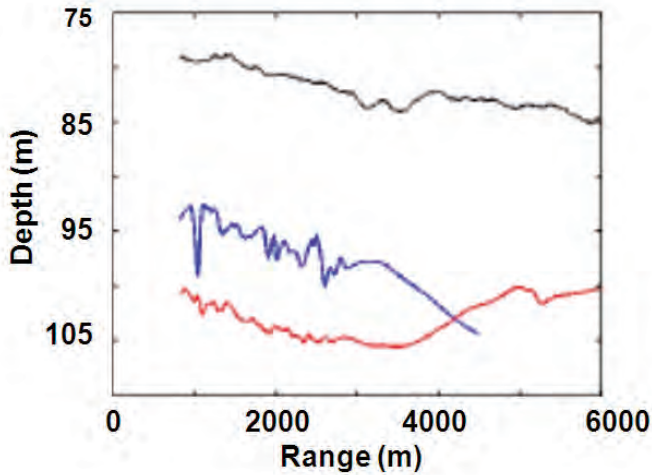


Figure 3. Chirp sonar depth profile from the SW06 experiment showing the depths of interfaces detected in the survey (upper curve: sea floor; middle curve: slow-speed erosive layer boundary; bottom curve: R-reflector)

The inverse problem in Eq. (7) is ill-posed and requires some form of regularisation to obtain a solution. Ballard et al. [16] introduced a simple approach for piece-wise regularisation that enabled solution of a discontinuous sound speed profile, and used it to invert a range-dependent sound speed profile from the SW06 data. The method requires *a priori* knowledge of the locations of sound speed discontinuities in the sub-bottom material. This information was obtained from chirp sonar surveys of the SW06 experimental sites before the experiment, and the resulting section in depth (converted from two-way sonar signal travel time) is shown in Figure 3. The combined inversion of modal wave number data and two-way travel time information was able to estimate the sound speed in the three different sediment layers that were defined by the sonar data. However, without this type of additional information, the perturbation inversion can generate only a smoothed approximation to the profile [16].

## MODEL-BASED INVERSION

Sophisticated numerical methods for solving non-linear geoacoustic inverse problems have been developed and implemented within the last two decades. The methods have been critically evaluated in workshops with simulated data [10, 11], and are in widespread use in applications with experimental data. The initial development of these methods was based on the use of matched field processing (MFP). The concept of MFP was known for a very long time, from the first simple experiments of Parvulescu and others at Hudson Laboratories that were reported in the mid 1960's [17] and the first formal paper by Homer Bucker in 1976 [18]. However, the method could not be applied effectively until modern numerical propagation models and fast computers with large storage capacity became available. The next section describes the background of MFP and the evolution of its use in ocean acoustics for source localisation and then geoacoustic inversion.

### Matched field processing

A harmonic sound source in the ocean creates a unique distribution of the acoustic field in range and depth that can be expressed in terms of the propagating modes in the waveguide:

$$P(r,z) = \frac{e^{i\pi/4}}{\sqrt{8\pi} \rho_0(z_s)} \sum_{m=1}^M Z_m(z_s) Z_m(z) \frac{\exp(ik_m r)}{\sqrt{k_m r}} \quad (8)$$

It can be seen from Eq. (8) that the spatial variation of the acoustic field contains information about the source/receiver geometry  $(r, z_s)$  and the waveguide model parameters that generate the modes.

Matched field processing was developed first as a method for extracting information about the source location from the spatial coherence of the acoustic field. In its most basic form, MFP compares measurements of the complex pressure  $P(r,z)$  at specific sensor locations with calculated replica fields  $Q(r,z)$  for the same locations. If the propagation model is correct (i.e., if the propagation model includes the correct physics of the problem), and if the physical model of the waveguide is a sufficiently accurate representation of the ocean environment, then the calculated field for the correct values of the true source depth and range  $(r_s, z_s)$  will be equal to the measured field  $P(r_s, z_s)$  (to within a complex constant). This simple description defines MFP in terms of physically intuitive comparisons between measured and calculated acoustic fields. It is useful to retain this very physical picture of MFP in order to understand the more formal development.

In analogy with a conventional beamformer, the comparison process can be quantified by projecting the calculated replicas of the acoustic field on the measured data. The output of the MF processor can then be expressed in terms of the normalized Bartlett correlation for a frequency  $\omega$ :

$$\begin{aligned} B(r,z;\omega) &= |Q^\dagger(r,z;\omega)P(r,z;\omega)|^2 / |Q(r,z;\omega)|^2 |P(r,z;\omega)|^2 \\ &= Q^\dagger(r,z;\omega)P(r,z;\omega)P^\dagger(r,z;\omega)Q(r,z;\omega) / |Q(r,z;\omega)|^2 |P(r,z;\omega)|^2 \end{aligned} \quad (9)$$

where  $P = [P_1, P_2, \dots, P_N]^T$  is the vector of measurements at

an array of  $N$  elements,  $Q = [Q_1, Q_2, \dots, Q_N]^T$  is the vector of calculated replicas for the array and  $\dagger$  denotes complex transpose. The quantity  $PP\dagger$  is the data covariance matrix that contains the relative phase information of the signal field across the array of sensors in the off-diagonal terms, as well as the signal power at each sensor in the diagonal terms. The difference between MFP and conventional beamforming is that the relative phase is determined from the full field solution to the wave equation instead of from plane waves.

The Bartlett processor described here is just one of many matched field processors that were developed and used for source localisation [19]. In all cases, the approach involved a systematic grid search to calculate an ambiguity surface of the matched field processor output over range and depth, as shown in Figure 4. This could be implemented very efficiently using normal mode propagation models because the environment model was constant for all points in the grid so that only one calculation of the field was needed. The true source location occurred at the ambiguity surface peak, assuming that the ocean waveguide environment model was correct.

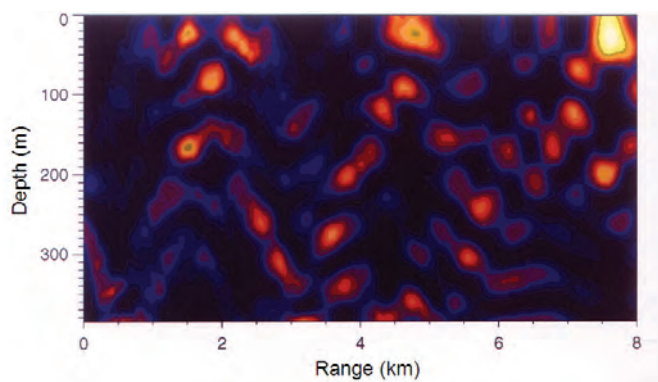


Figure 4. Matched field ambiguity surface for 45-Hz source from an experiment off the west coast of Vancouver Island, British Columbia. The peak at  $\sim 30$  m depth and 7.7 km range indicates the source location

The example shown in Figure 4 displays the Bartlett matched field ambiguity surface based on data from an experiment carried out in shallow water ( $\sim 400$  m) on the continental shelf off the coast of Vancouver Island, British Columbia. The ambiguity surface peak at a depth of  $\sim 30$  m and a range of 7.7 km indicates the location of the continuous wave 45-Hz source that was towed in the experiment. The sidelobes in the surface indicate locations of relatively high correlations. Since the propagation is bottom limited, there is a strong sidelobe at roughly half the distance to the source, approximately the range of the first bottom reflection for the shallow-angle propagating modes.

### Optimisation inversions

Although the source/receiver geometry is generally more sensitive in MFP, there is also sensitivity to the ocean bottom properties that can be exploited to estimate geoacoustic model parameters. This hierarchy in sensitivity of geometric and geoacoustic parameters was formalised in the concept

of focalisation by Collins and Kuperman [20]. Their work showed that an accurate source location could be obtained for ‘effective’ models of the ocean bottom that were not necessarily realistic. This result is not unexpected, since the inverse problem is non-unique and there are many models that can provide a good fit to the data in model-based inversions. However, the application of MFP for geoacoustic inversion did not follow directly. The reason was simply that the inversion process required a computationally expensive calculation of the acoustic field to assess each new parameterisation of a multi-parameter geoacoustic model, and this prohibited a simple grid search for most cases of realistic models. The breakthrough that enabled matched field inversion (MFI) came with the introduction of numerical search algorithms such as simulated annealing [21] and genetic algorithms [22] for efficient navigation of multi-dimensional model parameter spaces. These methods reduced the computation time of the search process that was implemented to assess the models. The inversions were initially cast in terms of optimisation algorithms that consisted of four basic components:

- A prior geoacoustic model for the ocean bottom environment
- An accurate method for calculating the replica acoustic fields
- A cost function for comparing the measured and calculated fields
- An efficient search method for navigating the multi-dimensional model parameter space

The form of the prior geoacoustic model determined the structure and properties of the model that was inverted, and so the design of the model required careful development. The model was based on knowledge of the local environment that was available from ‘ground truth’ information such as sediment cores and physical grab samples, and high resolution seismic and chirp sonar surveys. Model structure was generally based on homogeneous or gradient layers of sound speed, attenuation and density to represent the sediment material in the ocean bottom, and the distribution of model parameter values was assumed to be uniform within the bounds that were set. The water sound speed profile was usually taken from measurements at the experimental site and was assumed known in the inversion. The cost function was generally based on the Bartlett processor, although other measures such as the high resolution minimum variance processor were sometimes used [19]. Models that were tested in the search process were selected or rejected based on the change in the cost function. Convergence was controlled either by pre-selecting the number of iterations, or by a criterion that set a minimum value for the change of the cost function (e.g. [24]).

A number of highly efficient numerical search methods were developed and implemented in various applications with data. Inversions based on simulated annealing were reported in the early 1990s [23, 24]. Simulated annealing is an example of an approach based on importance sampling for efficiently navigating multi-dimensional model parameter spaces. By analogy with thermodynamic cooling, SA uses a Boltzmann criterion to accept models that do not decrease the cost function. This feature allows the search to move away from areas of local

minima in the model parameter space, thus enabling a more extensive search. The genetic algorithm that is distributed in the widely used SAGA software package is another example of a global search technique based on importance sampling [22]. A number of hybrid search methods were also developed that combined global and local search processes such as the downhill simplex method, e.g. simulated annealing and downhill simplex [25]; genetic algorithm and Gauss-Newton [26]; genetic algorithm and downhill simplex [27].

Results of optimisation inversions using simulated annealing were conventionally presented in terms of the annealing history of each model parameter during the search process. However, the annealing history shows only the rate at which the optimal values were obtained in the search process. Although the annealing rate gives a rough impression of which parameters are more sensitive in the inversion, it does not give a good indication of how well each parameter was estimated. A better but still qualitative sense of the hierarchy of sensitivities of the model parameters and a rough measure of the uncertainties of the estimated values can be obtained from a scatter plot of the cost function values for each model that was tested in the search process. Figure 5 shows scatter plots for two different model parameters. Scatter plots that appear like ‘tornadoes’ as in the left panel indicate well-estimated parameters with values that cluster in a small region of the allowed range. Those that appear broader at the base, as in the right panel, indicate less sensitive parameters that are not well estimated; the flatness of the display essentially indicates that the experimental data do not contain any useful information about the parameter.

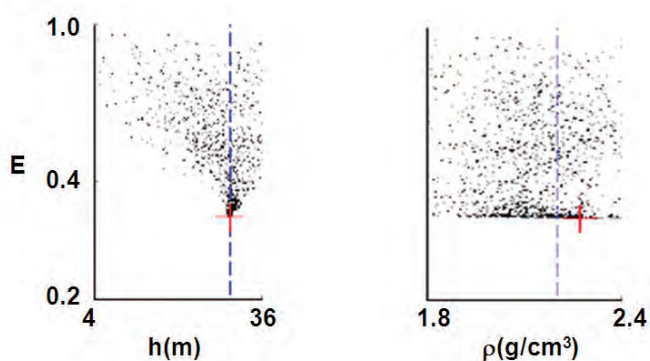


Figure 5. Typical scatter plots of cost function values ( $E = 1 - B(r, z; \omega)$ ) for two different geoacoustic model parameters. The left panel shows clustering of accepted models in a favoured region of the allowed range of values; the right panel shows a flat scatter indicating that no particular value of this parameter provides a better estimate than any other

Examination of scatter plots from optimisation inversions reveals the inherent weakness of the approach. Optimisation inversions always provide an ‘optimal’ estimate for each model parameter. However, it is usually the case for inversions with experimental data that some model parameters are insensitive, so that the ‘optimal’ values of those parameters do not significantly affect the acoustic field. As a result, inversions

can be over-parameterised, with meaningless estimates for some of the model parameters. In close scrutiny, optimisation inversions do not generate statistically valid measures of the errors in the estimated values, and consequently do not provide a complete solution to the inverse problem. However, it usually turns out that the spread of values obtained for a large number of optimisation runs (each one with different starting values) is contained within the error bounds of inversions carried out by Bayesian inference. Thus, the shape of the scatter plot generally gives a reasonable qualitative sense of the uncertainty of the estimate.

### Model parameter correlations

An inherent problem in geoacoustic inversion arises from the correlations that exist between model parameters. At the very least, this leads to inefficient searches in the inversions. Optimisation inversions addressed this problem by re-parameterising the initial set of model parameters during the initial stages of the inversion [28]. Although this enables more efficient navigation of the model parameter space in the search process and is widely used, it does not eliminate the basic problem. The fundamental issue of mismatch remains: due to the model parameter correlations, errors in the estimate of one parameter will affect the estimates of all the others.

A simple but striking example of model parameter mismatch is the acoustic ‘mirage’ in source localisation by MFP. D’Spain et al. [29] showed that the range and water depth were strongly correlated in matched field source localisation. If the water depth used in calculating the replica fields was in error, the range was shifted in a predictable way. Since water depth and source range are not known exactly in experiments, the uncertainty in these parameters generates errors in the estimates of all the other model parameters in matched field inversions. The impact of this type of mismatch could be reduced by including geometric parameters of the experimental arrangement in the inversions, at the expense of increased computation time in searching a greater number of model parameters. This approach was adopted by many researchers. It supplied a useful consistency check on the quality of the inversions, provided that the inversion generated accurate estimates of the geometric parameters. Another well known example of mismatch is the correlation between source range and sound frequency through the waveguide invariant [1]. Errors caused by this effect were encountered initially when it was common practice to use only single frequency data in the inversions. The use of multi-frequency data (multiple tones or broad band signals) mitigates the impact of this mismatch to some degree.

These examples of mismatch errors in model-based inversions stress the fundamental issue of non-uniqueness of the solution to the inverse problem. Some researchers reported attempts to generate probabilities of the parameter values from the models that were tested in the search process as a means to address the uncertainties of the estimated values [30, 31]. However, the full resolution of the inverse problem as a statistical inference process was provided by Dosso [32] who introduced Bayesian inference [33] for geoacoustic inversion in ocean acoustics.



# GEOACOUSTIC INVERSION BY STATISTICAL INFERENCE

## Bayesian inference

The Bayesian formulation of the matched field geoacoustic inverse problem follows from Bayes' relationship between measured data and a set of environmental model parameters that is expressed in terms of conditional probabilities:

$$P(\mathbf{m}|\mathbf{d})P(\mathbf{d}) = P(\mathbf{d}|\mathbf{m})P(\mathbf{m}) \quad (10)$$

Here,  $P(\mathbf{m}|\mathbf{d})$  is the conditional probability of the model given the data,  $P(\mathbf{d}|\mathbf{m})$  is the conditional probability of the data given a model  $\mathbf{m}$ , and  $P(\mathbf{m})$  is the prior information about the model  $\mathbf{m}$ . The quantity  $P(\mathbf{d})$  is the probability of the data, for the selected model parameterisation. If we assume that the model parameterisation is correct, then for observed data,  $P(\mathbf{d})=1$ . However, in general the correct parameterisation is not known, and  $P(\mathbf{d})$  can be considered as the likelihood of the parameterisation given the data.

In the Bayesian framework, the complete solution of the inverse problem is given by  $P(\mathbf{m}|\mathbf{d})$ , the *a posteriori* probability distribution (or PPD) of model parameter values. It is evident from Eq. (10) that Bayesian inversion involves an interaction between the information about the model that is contained in the data and the prior knowledge about the model. If there is no information in the data about a model parameter, the probability of that parameter is close to the original prior probability distribution. Otherwise, the final probability distribution is determined by the information contained in the data.

The relationship between the data and the set of environmental model parameters can be interpreted in terms of the mismatch between the measurement and a prediction of the measurement  $\mathbf{q}$  based on the model:

$$\mathbf{d} - \mathbf{q}(\mathbf{m}) = \mathbf{n} \quad (11)$$

The mismatch  $\mathbf{n}$  can be interpreted as noise that arises from either the uncertainty in the experimental data itself or theory errors owing to differences between the environmental model and the real earth, or differences caused by an inaccurate model of the physics of the problem (in this case, the wave equation). The statistical distribution of  $\mathbf{n}$  is generally not known.

Bayesian inversion is implemented by assuming that the conditional probability of the data for a given model,  $P(\mathbf{d}|\mathbf{m})$ , in Eq. (10) can be expressed in terms of a likelihood function of the data and model mismatch,  $L(\mathbf{m},\mathbf{d})$  for data:

$$L(\mathbf{m},\mathbf{d}) = \frac{1}{\pi^N |C_d|} \exp\{-[E(\mathbf{m},\mathbf{d})]\} \quad (12)$$

where  $C_d$  is the data error covariance matrix,  $N$  is the number of sensors and the data and model mismatch is defined as  $E(\mathbf{m},\mathbf{d})$ :

$$E(\mathbf{m},\mathbf{d}) = [(\mathbf{d} - \mathbf{q}(\mathbf{m}))^\dagger C_d^{-1} (\mathbf{d} - \mathbf{q}(\mathbf{m}))] \quad (13)$$

In many applications, the assumption is made that the covariance matrix is diagonal. However, this condition is not usually correct, and some attempt must be made to evaluate  $C_d$

in the inversion. This involves making assumptions about the statistics of the data mismatch distribution, and these must be verified by statistical tests [34, 35].

Although the complete solution of the inverse problem is given by the PPD, it is a multi-dimensional distribution that is difficult to visualise. Its interpretation in terms of model parameter estimates and their uncertainties involves computation of the properties of the PPD, such as the maximum *a posteriori* estimate (MAP), the mean values and covariances, and marginal probability distributions. Parameter uncertainties can be quantified in terms of credibility intervals, i.e. the  $\gamma\%$  highest probability density interval (HPD) that represents the minimum width interval that contains  $\gamma\%$  of the marginal probability distribution.

The Bayesian formulation is quite general, and the method can be applied to any of the types of data that are derived from the acoustic field. For the usual case in matched field inversion that the phase ( $\theta$ ) and amplitude ( $A$ ) of the source sound pressure are unknown, the modeled data can be expressed as

$$\mathbf{q}(\mathbf{m}) = A e^{i\theta} F_\omega(\mathbf{m}) \quad (14)$$

where  $F_\omega$  is the forward propagation model used to calculate the replica field at frequency  $\omega$  for the geoacoustic model  $\mathbf{m}$ . The dependence on the source can be removed by maximizing over  $\theta$  and  $A$  to obtain a misfit function that is given by the covariance-weighted Bartlett mismatch

$$E_\omega(\mathbf{m},\mathbf{d}) = \mathbf{d}_\omega^\dagger C_d^{-1} \mathbf{d}_\omega - \frac{|F_\omega(\mathbf{m}) C_d^{-1} \mathbf{d}_\omega|^2}{F_\omega^\dagger(\mathbf{m}) C_d^{-1} F_\omega(\mathbf{m})} \quad (15)$$

For multi-frequency data the different frequencies are usually combined incoherently, so that Eq. (12) becomes a product over the number of frequencies, and Eq. (15) becomes a summation.

## Limitations of matched field Bayesian inference

Inversions based on the Bayesian formulation were applied to experimental data from many different experiments, with remarkable successes in estimating geoacoustic profiles that compared favourably with ground truth information for the local environment [36-39]. However, most of the experiments were carried out at sites where the ocean environment was benign for MFI: constant water depth and minimal variability of the ocean sound speed profile and the sediment materials and structure over the track of the experiment. For these conditions, the inversions could be carried out assuming that the sound propagation was independent of range. An example of Bayesian inversion with experimental data from the SW06 experiment is discussed here that demonstrates the performance of the method, and reveals the fundamental limitations of MFI in strongly variable ocean environments [40].

The SW06 experimental site is strongly influenced by internal waves, eddies and fronts that are shed from the Gulf Stream that passes offshore along the coast of New Jersey. These features create a highly variable sound speed profile in the ocean, with short time scales of the order of minutes and spatial variability scales of the order of a few km. An example

of the sound speed variability at the site during the experiment is shown in Figure 6. The profiles were obtained from CTD (conductivity, temperature, salinity) measurements from the source ship at stations along the track of the experiment.

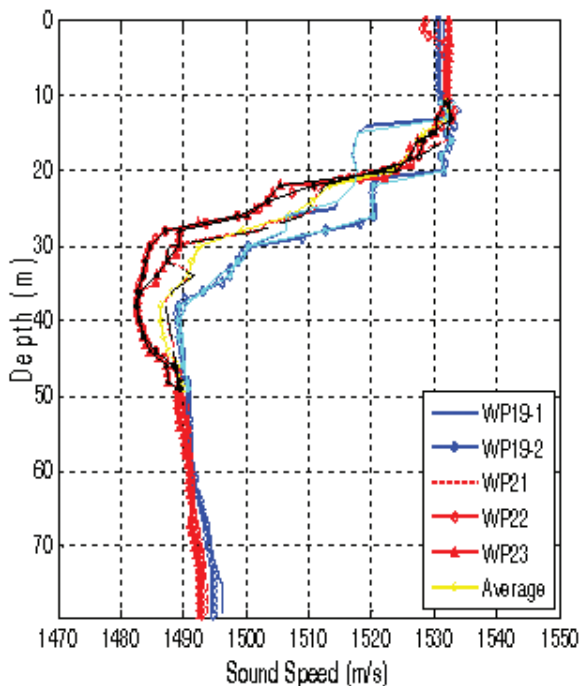


Figure 6. Sound speed profiles measured from CTDs deployed along the track from the SW06 experiment

The data used in the experiment were multiple CW tones transmitted from a ship that held station at a distance of 1 km from a bottom moored vertical line array. The array consisted of 16 hydrophones equal spaced at 3.75 m, with the bottommost sensor about 8.2 m above the sea floor. The water depth was ~79 m over the propagation path. Data from 7 CW tones over the frequency band 53–703 Hz were combined incoherently in the inversion.

The ocean environment in SW06 presented a significant challenge for MFI due to the strong spatial and temporal variability of the sound speed profile in the water over the experimental track. The conventional practice in MFI of using a single measured sound speed profile for the water column was ineffective for inverting the data. A simple demonstration of this problem is obtained from an ambiguity surface calculated for source localisation using one of the measured profiles. The true source location should be at 30 m and 1 km range, but as can be seen in Figure 7, the estimated location is near the ocean bottom and much closer in range. The ambiguity surface was calculated using 7 CW tones that were processed incoherently over frequency. In this case, the use of multiple frequencies was not effective in mitigating the mismatch caused by the unknown variation in the water sound speed profile, since the field could not be properly focussed at the receiver for any of the frequencies.

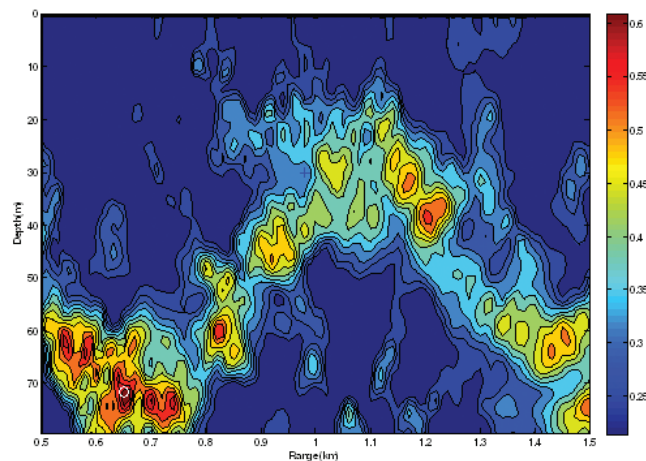


Figure 7. Ambiguity surface for multi-tone CW data from the SW06 experiment

To account for the variability, it was assumed that a single estimated profile would account for the changes in the water sound speed along the propagation path. The profile was modelled by empirical orthogonal functions (EOFs) to account for the observed variability in the profile, and the EOFs were included as unknowns in the inversion. Consequently, a total of 17 parameters were required in the inversion: 4 geometrical parameters of the experimental arrangement (source range and depth, water depth, and array tilt); 4 EOFs for the sound speed profile in the water; and 9 geoaoustic parameters of a single layer model of the bottom in which the sediment was modelled as a gradient layer for the sound speed and density over a halfspace basement (Figure 1). The local environment was assumed to be range independent in the inversion.

The inversion results are presented as marginal probability densities for the model parameters in Figure 8. Sensitive parameters that are well estimated have marginal densities that are tightly focused in a favoured region of the parameter bounds; the marginal densities for parameters for which there is little information in the data are flatter. These shapes are similar to the shapes of the scatter plots from optimization inversions for parameters with similar sensitivities. However, a statistically meaningful measure of the uncertainty can be derived from the Bayesian inference, such as the 95% HPD limits. As seen in the figure, the geometric parameters indicated by the dashed circles were highly sensitive in the inversion, and the estimated values compared very well with independent measurements of the range, source depth and bathymetry from the experiment. The 4 EOFs were also well estimated.

Marginal densities for the layer depth ( $H$ ), and top and bottom sound speed of the sediment layer,  $c_{p1}$  and  $c_{p2}$ , respectively and the sound speed in the basement half space,  $c_{pb}$ , (shown in the solid circles) were also tightly focused, indicating that these geoaoustic parameters were well estimated. However, the marginal densities for the other geoaoustic parameters were relatively flat, indicating that the data did not contain significant information about them.

The results shown in the figure are typical of those from other matched field inversions: the most sensitive parameters are



generally the sound speeds in the uppermost layers of sediment (within a few wavelengths of the sea floor). A particularly striking result from this inversion is the accurate estimate of sediment thickness. Ground truth chirp sonar surveys revealed a strong sub-bottom reflector at a depth of about 20 m that was ubiquitous over the experimental area. The inversion was also sensitive to a slow sound speed layer within the sediment above the basement reflector. Although the detailed structure within the sediment could not be resolved with these data, the presence of the low speed layer was inferred from the negative gradient of sound speed within the sediment.

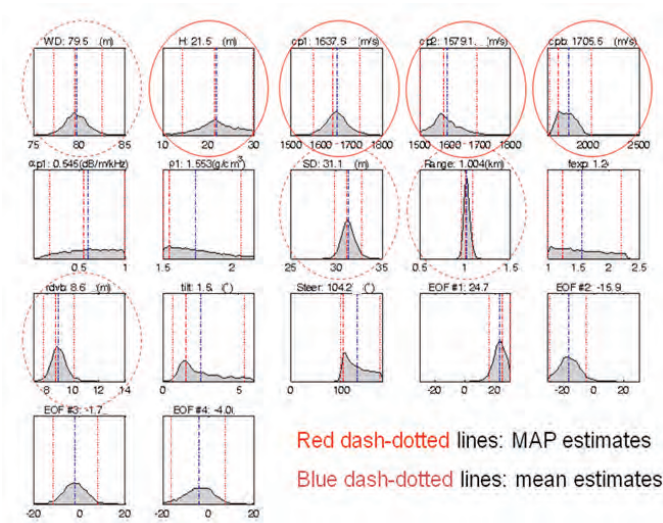


Figure 8. Marginal probability densities for the model parameters inverted from the SW06 data. The vertical dashed lines represent the 95% HPD limits. Red dash-dotted lines are MAP estimates, and blue dash-dotted lines are the mean estimates. The solid and broken circles indicate well estimated geoacoustic and geometric parameters, respectively

Attenuation is interpreted as an intrinsic loss in the sediment, and was modelled in this inversion as frequency dependent,  $\alpha_0(f/f_0)^\beta$ , where  $f_0 = 1$  kHz. The results indicated that the inversion with data from a range of 1 km was not sensitive to attenuation: the marginal densities for the constant,  $\alpha_{p1}$ , the exponent,  $f_{exp}$ , were flat. However, the experimental data are affected by other mechanisms that remove energy from the propagation plane, such as scattering. Since the loss accumulates with range, data from greater ranges likely contain more information about attenuation.

Other insight into the estimated model can be obtained from two-dimensional marginal densities. Displays such as shown in Figure 9 for the SW06 data reveal model parameter correlations, and provide added confidence about the quality of the estimated model. From the figure, there is a clear indication of the correlation between water depth (WD) and range, and also water depth and source depth (SD). The correlation between the water depth and first EOF shows the linkage between the waveguide depth and the sound speed profile in focussing the signal at the receiver. A negative sound speed gradient in the sediment layer is revealed in the correlation between the top

and bottom sound speeds of the layer ( $c_{p1}$  and  $c_{p2}$ ). Other pairs of parameters do not show any strong correlation, as would be expected for pairs such as water depth and the thickness of the sediment layer.

Although the inversion was successful in providing accurate estimates of the geoacoustic model, the overall success of the same approach for other data sets at longer ranges was not repeated. The success of the inversion reported here depended on the assumption that the sound speed variation in the water column could be represented by a single profile based on the observed sound speed variations. This assumption was not upheld for data from ranges of 3 km and 5 km from the same experiment. Oceanographic data from moored sensors revealed that internal waves passed through the experimental site when the longer range data were obtained. Knowledge of the full range dependence of the sound speed profile is required for inverting these data.

This example indicates the fundamental weakness of model-based inversions such as MFI. If the environmental variation cannot be modelled sufficiently accurately, the inversion will fail. However, the degree of variability that will allow simple assumptions such as a single profile is not known. And even for simple assumptions, the increased computational load of including additional model parameters as unknowns in the inversion is a significant drawback.

### Other challenges in model based inversions

Apart from the issues mentioned above, there are other challenges that need to be addressed in model based inversions. Most of the inversions reported to date have been restricted to low frequencies ( $< 1$  kHz) for which the sea floor and sub-bottom layer interfaces are assumed to be smooth. Inversions at higher frequencies must address rough surface scattering losses in modelling the acoustic field. The impact of shear wave propagation in the bottom has been considered in some inversions, but this issue is generally ignored. Another important issue is the assumption of 2-D sound propagation. In most cases, this assumption is valid. However, in experimental geometries that involve propagation across a sloping sea bottom such as along a continental shelf, 3-D propagation effects must be considered. An example reported by Jiang et al. demonstrated the impact of 3-D sound propagation on MFI at a site in the Florida Straits [41]. In this inversion, the sound refracted along the slope could be removed by spatial filtering since it was propagated in higher order modes with larger propagation angles. Otherwise, a 3-D sound propagation model is required [42].

Ocean sediments are porous media, and there has been significant research effort in developing theories of sound propagation in sediment materials. Among the most well known theories are the Biot theory [43, 44], and the more recent theories based on viscous grain shearing by Buckingham [45-47]. The critical issue for modelling sound propagation is the dispersion of sound speed and attenuation in sediments: experiments show that the frequency dependence of attenuation in sand sediments is non-linear within the low frequency band less than 5 kHz [48]. However in most applications of MFI, sound propagation has been modelled using viscous fluid models or in some cases

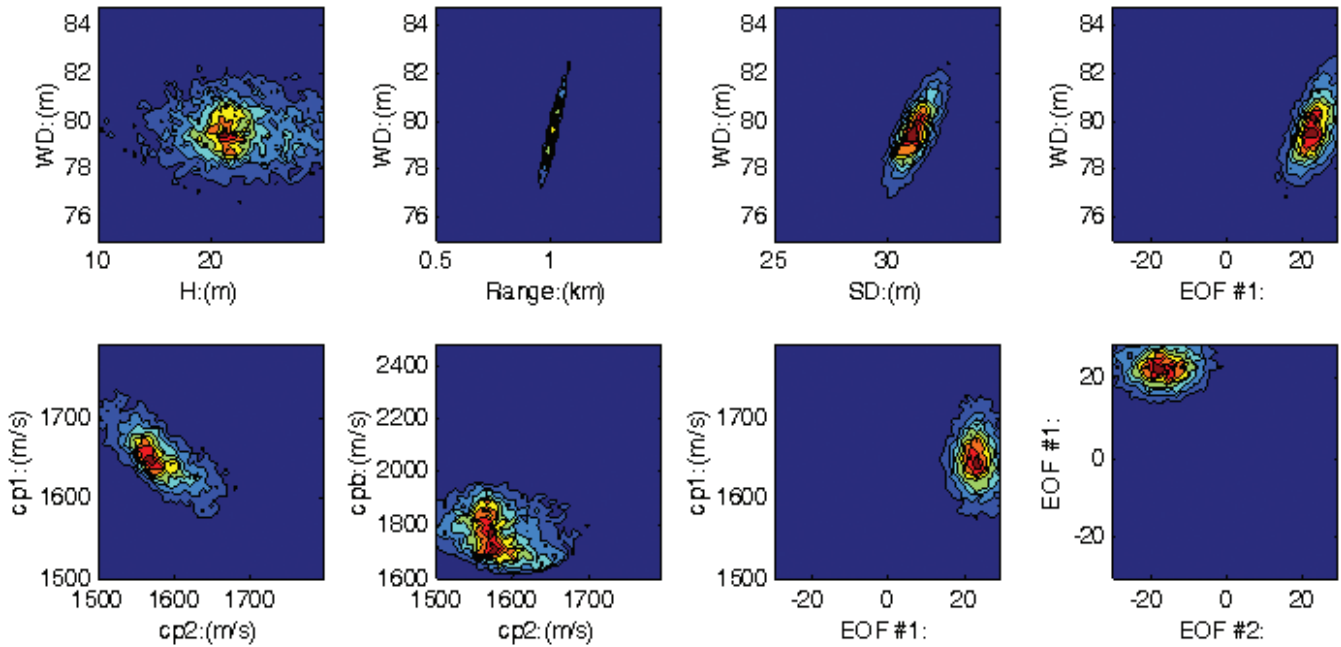


Figure 9. Two-dimensional marginal probability densities for the model parameters inverted from the SW06 data

visco-elastic models, both of which inherently assume linear frequency dependence for attenuation.

The impact of using more appropriate theories of sound propagation in marine sediments has not been examined extensively in MFI. One of the benefits of using the viscous grain shearing theory, for instance, may be in obtaining a more efficient set of model parameters for sampling the PPD. The theory provides analytic expressions for the sound speed, attenuation and density in terms of more fundamental physical parameters (such as porosity, compressional and shear grain contact stress) that are independent [47].

The inversions have generally assumed that the model developed from the prior information is correct. New work by Dettmer et al. [49, 50] has focused on removing the dependence on a specific form for the prior model in Bayesian inversions. Their research has introduced a method for allowing the inversion to select models during the inversion process. The method shows considerable promise, but at increased computational expense. Another approach using particle filters for applications in range dependent environments was implemented by Yardim et al. [51]. In analogy with a Kalman filter, the method tracks the source location and the changing ocean bottom environment.

## OTHER APPROACHES FOR GEOACOUSTIC INVERSION

There is no simple remedy to enable model-based approaches such as MFI for conditions in which there is insufficient knowledge of the waveguide environment. A reasonable alternative approach is to use quantities derived from the acoustic field in the inversion, instead of the measured pressure. Although this usually requires special signal

processing to extract the observable, there are clear benefits if modelling the observable is not sensitive to variability in ocean waveguide properties. One example is the use of travel time. Jiang et al. [52] reported a Bayesian inversion of relative travel times between sub-bottom and sea floor broadband signal arrivals to estimate sound speed and attenuation in the sediment. The experiment was designed to provide a tomographic sampling of the sediment using multiple source depths and a vertical hydrophone array at very short range. The data (shown in Figure 10 for a single source/receiver pair) are more robust to uncertainty in the water sound speed profile due to the relatively short range ( $\sim 200$  m), assuming that the sound speed profile is adequately sampled at the site during the experiment.

The sea bottom reflection coefficient derived from broadband data in an elegant experimental design has been used to invert fine structure of the sediment profile near the sea floor [53, 54]. However, the experimental geometry with a receiver very close to the sea floor requires calculation of reflection of a spherical wave to model the data correctly. Modal dispersion data have also been used in linearised inversions of time-frequency information [55]. This approach has the advantage of using a single receiver since the information is contained in the broad frequency band of the data. However, the technique is somewhat restricted to longer ranges to enable time resolution of the modes.

Perhaps the most novel approaches are those that make use of ambient noise. The use of ambient noise measured on a vertical array as a fathometer has been demonstrated by Siderius et al. [56]. Recently, Quijano extended this approach for geoacoustic inversion using the wind noise measured by the array as the sound source [57, 58]. The method inverts the

broadband reflection coefficient that is estimated from wind noise data on the array. The estimate of reflectivity is self-calibrated, and the reflection coefficient inversion is robust to uncertainty in the water sound speed profile. This is also true for the reflection coefficient inversions of controlled source data as proposed by Holland and Osler [53].

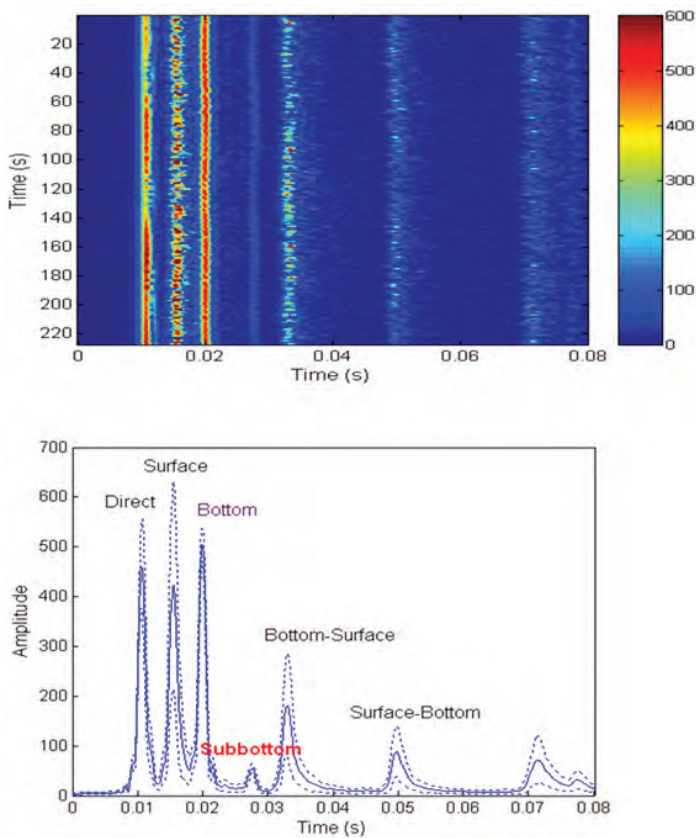


Figure 10. The multipath signal received at short range over a time of about 4 minutes. The top panel shows match filtered multipath signal from a 1-s chirp pulse over the band 1.5-2.5 kHz. The bottom panel shows the relative signal amplitudes over the time interval. Data are from the SW06 experiment

Finally, a promising technique that is robust to uncertainty in both the experimental geometry and the water sound speed profile was reported by Bonnel et al. [59, 60]. The method is based on estimating the modal dispersion from single hydrophone data using a signal processing technique known as warping. Although the use of modal dispersion data for estimating geoacoustic model parameters is not new, warping enables the inversion of relatively short range data for which the modes are not clearly separated in time. Warping transforms the non-linear dispersion relationship in the original time-frequency domain to single tones at frequencies near the Airy frequencies in the warped domain (Figure 11). It is evident from the figure that the range of the light bulb is not sufficiently great to resolve the modes in the original signal. The warping operation is reversible, so that the modes that are resolved in the warped domain can be filtered and transformed back to the original time-frequency space.

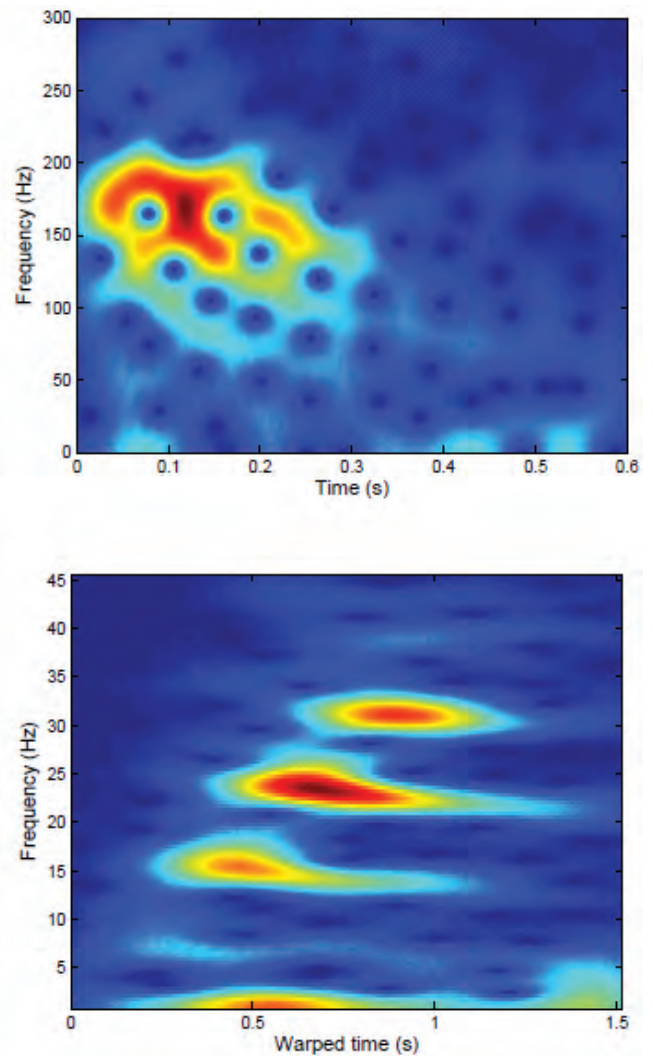


Figure 11. Left panel: original time-frequency dispersion of a light bulb shot deployed at a range of about 7 km in the SW06 experiment; right panel: the same signal transformed in the warped domain. Four modes are resolved at (warped) frequencies between 7 and 30 Hz

## SUMMARY

This paper reviewed the development of geoacoustic inversion in ocean acoustics as a statistical inference method. The inversion methods fall into two categories, linear and non-linear. Linear methods have been implemented using relationship between differences in horizontal wave numbers and sound speeds compared to an initial model. Linear methods have the advantage of efficient computational implementation, but the results are sensitive to the initial model. The widely used non-linear technique of matched field inversion was examined to display its advantages and discuss its fundamental limitations. The method is based on matched field processing in which model parameters are estimated by comparing measured data with calculated replicas of the data. The Bayesian formalism for matched field inversion provides the complete solution to the inverse problem: estimates of the model parameter values and statistically valid measures of their uncertainties are derived from the *a posteriori* probability



density. The marginal probabilities derived from the PPD indicate the degree to which the experimental data contain information about the model parameters. However, if there is uncertainty due to variability in the properties of the ocean environment, model-based inversions such as matched field inversion can fail.

New approaches that are robust to uncertain knowledge of the ocean properties and the experimental geometry provide some options for alternative methods for model-based inversion of geoacoustic model parameters. A few of these methods, such as time-frequency analysis of broadband data, reflection coefficient inversion and travel time tomography were briefly discussed.

## ACKNOWLEDGEMENTS

This research is supported by the Ocean Acoustics team of the US Office of Naval Research. Continuing support from Jeff Simmen, Ellen Livingston, Ben Reeder and Bob Headrick is gratefully appreciated.

## REFERENCES

- [1] L.M. Brekhovskikh and I.P. Lysanov, *Fundamentals of Ocean Acoustics, 3rd Edition*, Springer, Berlin, 2003
- [2] F.B. Jensen, W.A. Kuperman, M.B. Porter and H. Schmidt, *Computational Ocean Acoustics*, American Institute of Physics, Woodbury, New York, 1994
- [3] F.B. Jensen, and W.A. Kuperman, "Sound propagation in a wedge shaped ocean with a penetrable bottom", *Journal of the Acoustical Society of America* **67**, 1564-1566 (1981)
- [4] N.R. Chapman, "Modeling ocean-bottom reflection loss measurements with the plane-wave reflection coefficient", *Journal of the Acoustical Society of America* **73**, 1601-1607 (1983)
- [5] R.B. Evans and W.M. Carey, "Frequency dependence of sediment attenuation in two low frequency shallow water acoustic experimental data sets", *IEEE Journal of Oceanic Engineering* **23**, 439-447 (1998)
- [6] G.V. Frisk, "Inverse methods in ocean bottom acoustics", in *Oceanographic and Geophysical Tomography: Les Houches 1988*, edited by Y. Desubabies, A Tarantola and J. Zinn-Justin, North-Holland, Amsterdam, 1990, pp 439-437
- [7] A. Caiti, N.R. Chapman, J-P Hermand and S. Jesus, (editors) *Acoustic Sensing Techniques for the Shallow Water Environment*, Springer, Dordrecht (332 pages), 2006
- [8] N.R. Chapman, *Inverse problems in Underwater Acoustics, Handbook of Signal Processing in Acoustics*, D. Havelock, S. Kuwano and M. Vorlander, editors, Springer, New York, 2009, pp. 1723-1736
- [9] W. Menke, *Geophysical Data Analysis: Discrete Inverse Theory*, Academic Press, Orlando, 1987
- [10] A. Tolstoy, N.R. Chapman and G.E. Brooke, "Workshop '97: Benchmarking for geoacoustic inversion in shallow water", *Journal of Computational Acoustics* **6**, 1-28 (1998)
- [11] N.R. Chapman, S.A. Chin-Bing, D. King and R.B. Evans, "Benchmarking geoacoustic inversion methods for range dependent waveguides", *IEEE Journal of Oceanic Engineering* **28**, 320-330 (2003)
- [12] G.V. Frisk and J.F. Lynch, "Shallow water waveguide characterization using the Hankel transform", *Journal of the Acoustical Society of America* **76**, 205-211 (1984)
- [13] S.D. Rajan, J.F. Lynch and G.V. Frisk, "Perturbative inversion methods for obtaining bottom geoacoustic parameters in shallow water", *Journal of the Acoustical Society of America* **82**, 998-1017 (1987)
- [14] K.M. Becker and G.V. Frisk, "Evaluation of an autoregressive spectral estimator for modal wave number estimation in range-dependent shallow water waveguides", *Journal of the Acoustical Society of America* **120**, 1423-1434 (2006)
- [15] D.J. Tang, J.N. Moum, J.F. Lynch, P. Abbot, N.R. Chapman, P.H. Dahl, T.F. Duda, G. Gawarkiewicz, S. Glenn, J.A. Goff, H. Graber, J. Kemp, A. Maffei, J.D. Nash and A. Newhall, "Shallow Water '06: A joint acoustic propagation/nonlinear internal wave physics experiment", *Oceanography* **20**(4), 156-167 (2007)
- [16] M. Ballard, K.M. Becker and J.A. Goff, "Geoacoustic inversion for the New Jersey shelf: three dimensional sediment model", *IEEE Journal of Oceanic Engineering* **35**, 28-42 (2009)
- [17] A. Parvulescu, "Matched signal ("M.E.S.S.") processing in the ocean", *Journal of the Acoustical Society of America* **98**, 943-960 (1995)
- [18] H. Bucker, "Use of calculated sound fields and matched field processing to locate sound sources in shallow water", *Journal of the Acoustical Society of America* **59**, 368-373 (1976)
- [19] A. Tolstoy, *Matched Field Processing for Underwater Acoustics*, World Scientific Publishing, Singapore, 1993
- [20] M.D. Collins and W.A. Kuperman, "Focalization: Environmental focusing and source localization", *Journal of the Acoustical Society of America* **91**, 1410-1422 (1991)
- [21] A. Basu and L.N. Frazer, "Rapid Determination of the Critical Temperature in Simulated Annealing Inversion", *Science*, **21**, September 1990: 1409-1412 (1990)
- [22] P. Gerstoft, "Inversion of seismoacoustic data using genetic algorithms and a posteriori probability distributions", *Journal of the Acoustical Society of America* **95**, 770-782 (1994)
- [23] M.D. Collins, W.A. Kuperman and H. Schmidt, "Non-linear inversion for ocean bottom properties", *Journal of the Acoustical Society of America* **92**, 2770-2783 (1992)
- [24] C.E. Lindsay and N.R. Chapman, "Matched Field Inversion for Geoacoustic Model Parameters Using Adaptive Simulated Annealing", *IEEE Journal of Oceanic Engineering* **18**, 224-231 (1993)
- [25] S.E. Dosso, M.J. Wilmut and A-L. Lapinski, "An adaptive-hybrid algorithm for geoacoustic inversion", *IEEE Journal of Oceanic Engineering* **26**, 324-336 (2001)
- [26] P. Gerstoft, "Inversion of acoustic data using a combination of genetic algorithms and the Gauss-Newton approach", *Journal of the Acoustical Society of America* **97**, 2181-2190 (1995)
- [27] M. Musil, M.J. Wilmut and N.R. Chapman, "A hybrid simplex genetic algorithm for estimating geoacoustic properties using matched field inversion", *IEEE Journal of Oceanic Engineering* **24**, 358-369 (1999)
- [28] M.D. Collins and L. Fishman, "Efficient navigation of parameter landscapes", *Journal of the Acoustical Society of America* **98**, 1637-1644 (1995)
- [29] G.L.D. D'Spain, J.J. Murray, W.S. Hodgkiss, N.O. Booth and P. Schey, "Mirages in shallow water matched field processing", *Journal of the Acoustical Society of America* **105**, 3245-3265 (1998)
- [30] P. Gerstoft and C. Mecklenbrauker, "Ocean acoustic inversion with estimation of a posteriori probability distributions", *Journal of the Acoustical Society of America* **104**, 808-819 (1998)
- [31] L. Jaschke and N.R. Chapman, "Matched field inversion of broadband data using the Freeze Bath method", *Journal of the Acoustical Society of America* **106**, 1838-1851 (1999)

- [32] S.E. Dosso, "Quantifying uncertainties in geoacoustic inversion I: A fast Gibbs sampler approach", *Journal of the Acoustical Society of America* **111**, 128–142 (2002)
- [33] M.K. Sen and P.L. Stoffa, "Bayesian inference, Gibbs sampler and uncertainty estimation in geophysical inversion", *Geophysical Prospecting* **44**, 313–350 (1996)
- [34] S.E. Dosso, P.L. Nielsen and M.J. Wilmut, "Data error covariance in matched-field geoacoustic inversion", *Journal of the Acoustical Society of America* **119**, 208–219 (2006)
- [35] Y-M. Jiang, N.R. Chapman and M. Badiey, "Quantifying the uncertainty of a geoacoustic model for the new jersey shelf by inverting air gun data", *Journal of the Acoustical Society of America* **121**, 1879–1894 (2007)
- [36] Z.-H. Michaloupoulou, "Robust multi-tonal matched field inversion: A coherent approach", *Journal of the Acoustical Society of America* **104**, 163–170 (1998)
- [37] D.P. Knobles, R.A. Koch, L.A. Thompson, K.C. Focke and P.E. Eisman, "Broadband sound propagation in shallow water and geoacoustic inversion", *Journal of the Acoustical Society of America* **113**, 205–222 (2003)
- [38] D.J. Battle, P. Gerstoft, W.S. Hodgkiss, W.A. Kuperman and P.L. Nielsen, "Bayesian model selection applied to self-noise geoacoustic inversion", *Journal of the Acoustical Society of America* **116**, 2043–2056 (2004)
- [39] R.A. Koch and D.P. Knobles, "Geoacoustic inversion with ships as sources", *Journal of the Acoustical Society of America* **117**, 626–637 (2005)
- [40] Y-M. Jiang and N.R. Chapman, "The impact of ocean sound speed variability on the uncertainty of geoacoustic parameter estimates", *Journal of the Acoustical Society of America* **125**, 2881–2895 (2009)
- [41] Y-M. Jiang, N.R. Chapman and H.A. DeFerrari, "Geoacoustic inversion of broadband data by matched beam processing", *Journal of the Acoustical Society of America* **119**, 3707–3716 (2006)
- [42] F. Sturm, S. Ivansson, Y-M. Jiang and N.R. Chapman, "Numerical investigation of out-of-plane sound propagation in a shallow water experiment", *Journal of the Acoustical Society of America* **123**, EL155–EL160 (2008)
- [43] M.A. Biot, "Theory of propagation of elastic waves in a fluid-saturated porous solid. i. low-frequency range", *Journal of the Acoustical Society of America* **28**, 168–178 (1956)
- [44] M.A. Biot, "Generalized theory of acoustic propagation in porous dissipative media", *Journal of the Acoustical Society of America* **34**, 1254–1264 (1962)
- [45] M.J. Buckingham, "Theory of acoustic attenuation, dispersion, and pulse propagation in unconsolidated granular materials including marine sediments", *Journal of the Acoustical Society of America* **102**, 2579–2596 (1997)
- [46] M.J. Buckingham, "Theory of compressional and transverse wave propagation in consolidated porous media", *Journal of the Acoustical Society of America* **106**, 575–581 (1999)
- [47] M.J. Buckingham, "On pore-fluid viscosity and the wave properties of saturated granular materials including marine sediments", *Journal of the Acoustical Society of America* **122**, 1486–1501 (2007)
- [48] J.-X. Zhou, X.-Z. Zhang, and D. P. Knobles, "Low-frequency geoacoustic model for the effective properties of sandy seabottoms", *Journal of the Acoustical Society of America* **125**, 2847–2866 (2009)
- [49] J. Dettmer, S.E. Dosso and C.W. Holland, "Sequential trans-dimensional Monte Carlo for range-dependent geoacoustic inversion", *Journal of the Acoustical Society of America* **129**, 1794–1806 (2011)
- [50] J. Dettmer and S.E. Dosso, "Trans-dimensional matched-field geoacoustic inversion with hierarchical error models and interacting Markov chains", *Journal of the Acoustical Society of America* **132**, 2239–2250 (2012)
- [51] C. Yardim, P. Gerstoft and W.S. Hodgkiss, "Geoacoustic and source tracking using particle filtering: Experimental results", *Journal of the Acoustical Society of America* **128**, 75–87 (2010)
- [52] Y-M Jiang, N.R. Chapman and P. Gerstoft, "Estimation of marine sediment properties using a hybrid differential evolution method", *IEEE Journal of Oceanic Engineering* **35**, 59–69 (2010)
- [53] C.W. Holland and J. Osler, "High-resolution geoacoustic inversion in shallow water: A joint time- and frequency-domain technique", *Journal of the Acoustical Society of America* **107**, 1263–1279 (2000)
- [54] C.W. Holland, J. Dettmer and S.E. Dosso, "Remote sensing of sediment density and velocity gradients in the transition layer", *Journal of the Acoustical Society of America* **118**, 163–177 (2005)
- [55] G. Potty, J. Miller and J.F. Lynch, "Inversion for sediment geoacoustic properties at the New England Bight", *Journal of the Acoustical Society of America* **114**, 1874–1887 (2003)
- [56] M. Siderius, C.H. Harrison and M.B. Porter, "A passive fathometer technique for imaging seabed layering using ambient noise", *Journal of the Acoustical Society of America* **120**, 1315–1323 (2006)
- [57] J.E. Quijano, S.E. Dosso, J. Dettmer, M. Siderius, L.M. Zurk and C.H. Harrison, "Bayesian geoacoustic inversion using wind-driven ambient noise", *Journal of the Acoustical Society of America* **131**, 2658–2667 (2012)
- [58] J.E. Quijano, S.E. Dosso, J. Dettmer, L.M. Zurk and M. Siderius, "Trans-dimensional geoacoustic inversion of wind-driven ambient noise", *Journal of the Acoustical Society of America* **133**, EL47–EL53 (2012)
- [59] J. Bonnel, C. Gervaise, P. Roux, B. Nicolas and J. Mars, "Modal depth function estimation using time-frequency analysis", *Journal of the Acoustical Society of America* **130**, 61–71 (2011)
- [60] J. Bonnel and N.R. Chapman, "Geoacoustic inversion in a dispersive waveguide using warping operators", *Journal of the Acoustical Society of America* **130**, EL101–EL107 (2011)

